e-ISSN 3050-9645
p-ISSN 2795-3274

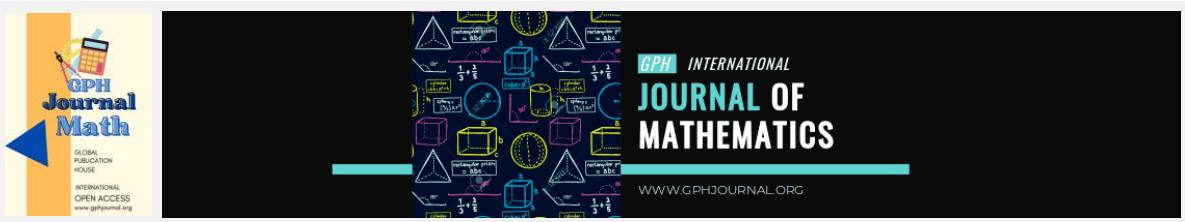

10.5281/zenodo.15630427 Vol. 8 Issue 04 April - 2025 Manuscript ID: #1946

Semi-Analytical Solution of Fractional Order Mathematical Model of COVID-19 via Atangana Baleanu- Caputor Derivative

I. G. Ezugorie[1], M. O. Ezugorie[2], B. C. Agbata[3]

[1]*Department of Industrial Mathematics/ Applied Statics, Enugu State University of Science and Technology, Enugu, Nigeria*

[2]*Department of Mathematics, Faculty of Physical Science, University of Nigeria, Nsukka, Nigeria*

[3]*Department of Mathematics and Statistics, Faculty of Science, Confluence University of Science and Technology, Osara, Nigeria*

Corresponding Author: agbatabc@custech.edu.ng

Abstract

COVID-19, caused by the novel coronavirus SARS-CoV-2, has had a profound global impact due to its high transmission rate and evolving clinical profile. Understanding its spread and identifying effective intervention strategies remain critical for public health planning. In this study, we develop a deterministic compartmental model to explore the transmission dynamics of COVID-19, incorporating a fractional-order derivative to account for memory effects inherent in disease progression. The human population is divided into six epidemiological compartments: susceptible, exposed, infected, under treatment, deceased, and recovered individuals. To more accurately reflect the temporal and cumulative effects of infection, we applied the Atangana–Baleanu–Caputo (ABC) fractional-order derivative, which improves the model's capacity to capture long-term dependencies often overlooked in classical models. A semi-analytical solution is derived using this approach. Stability analysis reveals that the disease-free equilibrium is locally asymptotically stable when the basic reproduction number is less than one, and unstable when othrwise. Through numerical simulations, it showed that reducing the contact rate and enhancing treatment interventions significantly lower infection prevalence and increase recovery rate. The findings highlight the effectiveness of timely treatment and behavioral control measures in curbing COVID-19 transmission. We recommend the continued enforcement of public health strategies such as reducing human-to-human contact, improving treatment accessibility, and increasing vaccine coverage. The proposed fractional-order model provides a more realistic framework for studying infectious diseases with memory-driven dynamics and can be adapted for future epidemic preparedness

Keywords and phrases:

COVID-19, Atangana–Baleanu–Caputo derivative, Basic reproduction number, Numerical simulation, Mathematical modeling.

How to cite: Ezugorie, I. G., Ezugorie, M. O., & Agbata, B. C. (2025). Semi-Analytical Solution of Fractional –Order Mathematical Model of COVID-19 Via Atangana Baleanu- Caputor Derivative. *GPH-International Journal of Mathematics*, 8(4), 01-20. https://doi.org/10.5281/zenodo.15630427

1. Introduction

The coronavirus disease 2019 (COVID-19), caused by the severe acute respiratory syndrome coronavirus 2 (SARS-CoV-2), has dramatically impacted global health systems and societies since its emergence. Despite widespread vaccination efforts, the virus continues to evolve, giving rise to new variants that challenge existing public health strategies [13][19]. The rapid spread and transmission dynamics of COVID-19 have necessitated continual monitoring and updating of vaccine formulations to maintain effectiveness against emerging strains, including the recent XBB.1.5 and JN.1 subvariants [8][22]. These viral evolutions have underscored the need for adaptive vaccination programs and real-time epidemiological modeling to inform public health responses [21].Vaccination remains the cornerstone in controlling COVID-19, with booster doses improving immunity, especially among vulnerable populations. Recent studies report that updated vaccines administered during the 2024–2025 season offer improved protection against circulating variants [2][20]. However, vaccine uptake varies globally, influenced by public perceptions, access, and evolving guidance from health authorities such as the CDC [4][9]. Furthermore, the development of needle-free vaccine delivery systems promises to enhance acceptance and facilitate mass immunization efforts in the near future [18]. Scientific evidence also supports the effectiveness of single mRNA vaccine doses in individuals with prior infections, demonstrating flexibility in immunization strategies [16]. Despite these advances, COVID-19 has given rise to long-term health complications, commonly referred to as Long COVID. This condition encompasses persistent symptoms such as fatigue, respiratory issues, and organ dysfunction, which can severely impact quality of life [6][10][17]. Recent research has begun elucidating the underlying pathophysiology of Long COVID, linking it to immune dysregulation and vascular damage [10][17]. Addressing these long-term sequelae is critical for healthcare planning and resource allocation in the post-pandemic era, as the burden on healthcare systems persists beyond the acute phase of infection.

The situation in Nigeria exemplifies the multifaceted challenges faced by countries in managing COVID-19 transmission. Socioeconomic factors, population density, and healthcare infrastructure influence the pandemic's trajectory, complicating containment efforts [21]. Modeling studies tailored to Nigeria's context have provided insights into transmission dynamics and the potential impact of vaccination campaigns and non-pharmaceutical interventions [21]. These models inform policymakers in designing effective strategies that balance public health priorities with socioeconomic considerations. Moreover, localized data highlight the need for continued surveillance and targeted vaccination efforts to curb outbreaks and mitigate long-term impacts.The evolving landscape of COVID-19 demands sustained scientific vigilance and public health innovation. The virus’s ability to mutate necessitates updated vaccines and adaptive immunization strategies [8][19]. Long COVID presents a growing healthcare challenge requiring focused clinical research and patient care initiatives [6][17]. Country-specific models, such as those developed for Nigeria, are essential for guiding tailored responses [21]. As vaccine technologies advance and global vaccination coverage improves, continued collaboration and research remain paramount to overcoming the COVID-19 pandemic and its lasting consequences.

[30] formulated a fractional-order influenza model using the Atangana–Baleanu–Caputo (ABC) derivative to incorporate memory effects in the disease progression. The model was tested against weekly influenza data from Saudi Arabia, and they s compared it with models based on Caputo–Fabrizio and classical Caputo derivatives. The analysis involved stability checks and fitting the model to actual epidemic data using standard error metrics such as

Root Mean Square Error (RMSE) and Mean Absolute Error (MAE). The ABC-based model showed superior accuracy in predicting the epidemic peak and tail dynamics. The study concluded that incorporating the ABC derivative provided a more realistic and flexible framework for epidemic modeling due to its non-local and non-singular properties. [31] developed a SEAIR (Susceptible–Exposed–Asymptomatic–Infectious–Recovered) model governed by the ABC fractional derivative. The study focused on analyzing the impact of memory and optimal control strategies on disease transmission. They proved mathematical properties including existence, uniqueness, positivity, and global stability of equilibria. Using the Toufik–Atangana numerical scheme, they simulated various fractional orders and tested different control interventions applied at varying intensities. Results indicated that a lower fractional order prolonged the epidemic's spread, allowing interventions more time to be effective. The study emphasized the critical role of early and sustained optimal control measures in mitigating disease transmission in fractional systems. [32] presented a fractional-order Zika virus model using a fractal ABC-Caputo derivative with a Mittag-Leffler kernel. The model included both human and mosquito compartments and captured the complexity of Zika transmission. Using fixed-point theory, the authors proved the model's stability and uniqueness. Numerical experiments revealed that as the fractional order decreased, the infection dynamics changed substantially, with slower peaks and longer persistence of the virus. The results demonstrated that fractional models, particularly with the ABC-Caputo derivative, provided a more nuanced understanding of vector-borne disease dynamics. The study concluded that incorporating fractal-fractional derivatives enabled more accurate epidemiological predictions and informed control planning.

[33] proposed a co-infection model that combined malaria and COVID-19 transmission within a single ABC fractional framework. The model consisted of several compartments, including human and mosquito populations. Mathematical analysis showed the existence and uniqueness of solutions, and reproduction numbers were derived for both diseases. Stability conditions were explored, and the model was simulated using a two-step Lagrange interpolation numerical scheme. Simulations indicated that interventions targeting one disease had a significant impact on the other due to shared pathways and host dynamics. It was concluded that ABC-based modeling of co-infections helped capture inter-disease feedback and could inform integrated public health strategies. The primary objective of this study is to develop and analyze a fractional-order deterministic compartmental model for COVID-19 transmission that incorporates memory effects via the Atangana–Baleanu–Caputo (ABC) derivative. This approach aimed to better capture the temporal dynamics of disease progression and assess the impact of various intervention strategies on the spread and control of the infection.

2. Preliminaries

Definition 2.1. On the interval $\beta \in [0, 1]$, by taking the function $f \in H^1(a,b), b > a,$ so that ABC derivative is given by ${}^{ABC}_{a}D^{\beta}_{\chi} f(\chi) = \frac{Z(\chi)}{1-\beta}\int_a^{\beta} f'(\theta) E_{\beta}\left[-\beta\frac{(\chi-\theta)^{\beta}}{1-\beta}\right] d\theta,$

With $Z(0) = Z(1) = 1$ [24], where $Z(\beta)$ is a normalization function.

Definition 2.2. [24] On the interval $\beta \in [0, 1]$, by taking the function $f \in H^1(a,b), b > a,$ which is not differentiable, hence the Atangana-Baleanu fractional derivative in Riemann-Liouville sense is defined as

$$ {}^{ABC}_{a}D^{\beta}_{\chi} f(\chi) = \frac{Z(\chi)}{1-\beta}\frac{d}{d\chi}\int_a^{\beta} f'(\theta)E_{\beta}\left[-\beta\frac{(\chi-\theta)^{\beta}}{1-\beta}\right]d\theta, $$

Definition 2.2. The ABC fractional derivative for the fractional integral of order β is given by

$$ {}^{AB}_{a}I^{\beta}_{\chi} f(\chi) = \frac{1-\beta}{\mathrm{A}(\beta)} f(t) + \frac{\beta}{\mathrm{A}(\beta)\Gamma(\beta)}\int_a^{\beta} f(\mathrm{y})(\chi-y)^{\beta-1}dy, $$

If $\beta = 0$ and $\beta = 1$, the initial function and ordinary integral are obtained, below.

In the next sections, we will investigate the Laplace transform operators and applied fundamental theorems associated with these derivatives. The connection between these operators and the Laplace Transform will be established.

$$ \mathcal{L}\left\{ {}^{ABR}_{0}D^{\beta}_{\chi}[f(\chi)]\right\}(l) = \frac{L(\beta)}{1-\beta}\frac{l^{\beta}\mathcal{L}\{f(\chi)\}(l)}{l^{\chi}+\frac{\beta}{1-\beta}} $$

and

$$ \mathcal{L}\left\{ {}^{ABC}_{0}D^{\beta}_{\chi}[f(\chi)]\right\}(l) = \frac{V(\beta)}{1-\beta}\frac{l^{\beta}\mathcal{L}\{f(\chi)\}(l) - l^{\beta-1}f(0)}{l^{\beta}+\frac{\beta}{1-\beta}} $$

Theorem 2.1. [25] Consider the close interval [a, b] and use ^{g} to represent a continuous function defined on it. we establish the following inequality, which is true for any point lies in [a, b]:

$$ \left\| {}^{ABR}_{0}D^{\beta}_{\chi}[f(\chi)]\right\| < \frac{V(\beta)}{1-\beta}\|f(\theta)\|, $$

Where $\|f(\theta)\| = \max_{a\le\chi\le b}|f(\theta)|$.

Theorem 2.2 [24] The *Riemann-Liouville* and Caputo types of Atangana-Baleanu derivative exhibit the Lipchitz condition, which is best defined as given below

$$ \left\| {}^{ABR}_{0}D^{\beta}_{\chi}[f(\chi)] - {}^{ABR}_{0}D^{\beta}_{\chi}[g(\chi)]\right\| \le H\|f(\chi)-g(\chi)\|. $$

And

$$ \left\| {}^{ABC}_{0}D^{\beta}_{\chi}[f(\chi)] - {}^{ABC}_{0}D^{\beta}_{\chi}[g(\chi)]\right\| = H\|f(\chi)-g(\chi)\|. $$

3. Methodology

3.1 Model Formulation

In this study, a mathematical model that captures how COVID-19 spreads through a population by categorizing individuals into groups based on their health status or role in the outbreak is formulated . The model uses differential equations to track how people move between these groups—such as from susceptible to infected over time. This approach allows for a detailed simulation of the pandemic's course and helps evaluate the potential impact of different public health interventions. The total human population is divided into six

epidemiological compartments: susceptible individuals S(t), exposed individuals E(t),, infected individuals I(t), deceased individuals D(t), individuals receiving treatment T(t), and recovered individuals R(t). Let Λ denote the recruitment rate, which adds new individuals to the susceptible class. The number of susceptible individuals decreases due to infection and natural causes at the rate λ , while exposed individuals progress to the infected class at a rate ε_1. The treatment rate and disease-induced death rate are denoted by ω and α_1 respectively, where γ represents the recovery rate of infected individuals, and α_2 corresponds to the burial rate of the deceased population. All compartments, except the deceased, are also reduced by the natural death rate μ\mu. Based on the model descriptions and Figure 1, the system is governed by the following set of differential equations.

3.2 Model Equations

$$\begin{aligned}
\frac{dS}{dt} &= \Lambda - (\lambda + \mu)S, \\
\frac{dE}{dt} &= \lambda S - (\varepsilon_1 + \mu)E, \\
\frac{dI}{dt} &= \varepsilon_1 E - (\alpha_1 + \omega + \mu)I, \\
\frac{dT}{dt} &= \omega I - (\alpha_1 + \mu)T, \\
\frac{dD}{dt} &= \alpha_1 I + \alpha_1 T - \alpha_2 D, \\
\frac{dR}{dtS} &= \gamma T - \mu R. \qquad (1)
\end{aligned}$$

The force of infection of the covid-19 model in (1) is given as:

Where $\lambda = \dfrac{\phi(\mathrm{I}+\mathrm{D}+\mathrm{T})}{N}$

Since fractional-order derivatives more accurately capture the dynamics of epidemiological patterns compared to classical derivatives, we reformulate the COVID-19 model (1) using the Atangana–Baleanu–Caputo (ABC) fractional derivative as follows:

$$\begin{aligned}
{}^{ABC}_{0}D^{\beta}_{\chi}S(\chi) &= \Lambda - (\lambda + \mu)S, \\
{}^{ABC}_{0}D^{\beta}_{\chi}E(\chi) &= \lambda S - (\varepsilon_1 + \mu)E, \\
{}^{ABC}_{0}D^{\beta}_{\chi}I(\chi) &= \varepsilon_1 E - (\alpha_1 + \omega + \mu)I, \\
{}^{ABC}_{0}D^{\beta}_{\chi}T(\chi) &= \omega I - (\alpha_1 + \mu)T, \\
{}^{ABC}_{0}D^{\beta}_{\chi}D(\chi) &= \alpha_1 I + \alpha_1 T - \alpha_2 D, \\
{}^{ABC}_{0}D^{\beta}_{\chi}R(\chi) &= \gamma T - \mu R. \qquad (2)
\end{aligned}$$

Subject to initial conditions

$$S(0)=S_0,\ E(0)=E_0,\ I(0)=I_0,\ T(0)=T_0,\ D(0)=D_0,\ R(0)=R_0.$$

4. Existence and uniqueness of solutions of model

Solving nonlinear equations is a well-known challenge in differential calculus, especially when dealing with complex systems like the fractional-order model explored in this study. Due to the model's high degree of nonlinearity, finding exact solutions becomes particularly difficult. Therefore, our main focus shifts to establishing whether solutions to model (2) actually exist and whether they are unique. To tackle this, we apply the fixed point theorem, a widely used mathematical tool for proving the existence and uniqueness of solutions in nonlinear systems [24, 25, 26]. This approach not only helps confirm the model's mathematical soundness but also provides deeper insights into the behavior of the system. On the interval ^{q} ,suppose that $p=K(g)\times K(g),$, where the Banach space $K(g)$ of continuous real value functions is defined with the norm

$$\|S,E,I,T,D,R\|=\|S\|+\|E\|+\|I\|+\|T\|+\|D\|+\|R\|.$$

Where;

$$\|S\|=\sup\{|S(\chi)|:\chi\in g\},$$
$$\|E\|=\sup\{|E(\chi)|:\chi\in g\},$$
$$\|I\|=\sup\{|I(\chi)|:\chi\in g\},$$
$$\|T\|=\sup\{|T(\chi)|:\chi\in g\},$$
$$\|D\|=\sup\{|D(\chi)|:\chi\in g\},$$
$$\|R\|=\sup\{|R(\chi)|:\chi\in g\}.$$

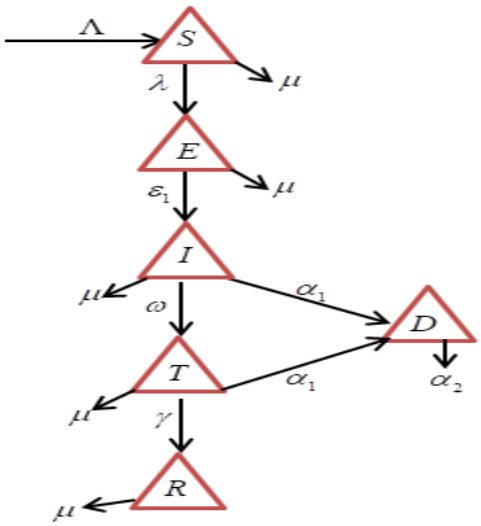

Figure 1: Schematic diagram for the covid-19 model

The model (2) is transformed into the following equation by taking the Atangana-Baleanu fractional-order derivatives.

$$
\begin{aligned}
S(\chi)-S(0)&=\frac{1-\beta}{\mathrm{A}(\beta)}\{\Lambda-(\lambda+\mu)S\}\\
&\quad+\frac{\beta}{\mathrm{A}(\beta)\Gamma(\chi)}\int_0^{\chi}(\chi-y)^{\beta-1}\{\Lambda-(\lambda+\mu)S\}\,dy\\
E(\chi)-E(0)&=\frac{1-\beta}{\mathrm{A}(\beta)}\{\lambda S-(\varepsilon_1+\mu)E\}\\
&\quad+\frac{\beta}{\mathrm{A}(\beta)\Gamma(\chi)}\int_0^{\chi}(\chi-y)^{\beta-1}\{\lambda S-(\varepsilon_1+\mu)E\}\,dy\\
I(\chi)-I(0)&=\frac{1-\beta}{\mathrm{A}(\beta)}\{\varepsilon_1 E-(\alpha_1+\omega+\mu)I\}\\
&\quad+\frac{\beta}{\mathrm{A}(\beta)\Gamma(\chi)}\int_0^{\chi}(\chi-y)^{\beta-1}\{\varepsilon_1 E-(\alpha_1+\omega+\mu)I\}\,dy\\
T(\chi)-T(0)&=\frac{1-\beta}{\mathrm{A}(\beta)}\{\omega I-(\alpha_1+\mu)T\}\\
&\quad+\frac{\beta}{\mathrm{A}(\beta)\Gamma(\chi)}\int_0^{\chi}(\chi-y)^{\beta-1}\{\omega I-(\alpha_1+\mu)T\}\,dy\\
D(\chi)-D(0)&=\frac{1-\beta}{\mathrm{A}(\beta)}\{\alpha_1 I+\alpha_1 T-\alpha_2 D\}\\
&\quad+\frac{\beta}{\mathrm{A}(\beta)\Gamma(\chi)}\int_0^{\chi}(\chi-y)^{\beta-1}\{\alpha_1 I+\alpha_1 T-\alpha_2 D\}\,dy\\
R(\chi)-R(0)&=\frac{1-\beta}{\mathrm{A}(\beta)}\{\gamma T-\mu R\}\\
&\quad+\frac{\beta}{\mathrm{A}(\beta)\Gamma(\chi)}\int_0^{\chi}(\chi-y)^{\beta-1}\{\gamma T-\mu R\}\,dy
\end{aligned}
\tag{3}
$$

Simplifying (3), we have

$$
\begin{aligned}
K_1(\chi,\ S)&=\Lambda-(\lambda+\mu)S,\\
K_2(\chi,\ E)&=\lambda S-(\varepsilon_1+\mu)E,\\
K_3(\chi,\ I)&=\varepsilon_1 E-(\alpha_1+\omega+\mu)I,\\
K_4(\chi,\ T)&=\omega I-(\alpha_1+\mu)T,\\
K_5(\chi,\ D)&=\alpha_1 I+\alpha_1 T-\alpha_2 D,\\
K_6(\chi,\ R)&=\gamma T-\mu R.
\end{aligned}
$$

Theorem 4.1. If the aforementioned inequality holds:

$0\le\phi_i<1,\quad \text{for } i=1,2,3,...,6$

Then the kernels k_1,k_2,k_3,k_4,k_5,k_6 satisfy the Lipschitz condition and hence, a contradiction

Proof.

By taking the kernel $\kappa_1(\chi,\ S)=\Lambda-(\lambda+\mu)S$. Let S and S_1 be any two functions, so that :

$$\begin{aligned}\left\|\kappa_1(\chi,\ S(\chi))-\kappa_1(\chi,\ S_1(\chi))\right\| &= \left\|\Lambda-\lambda S+\mu S-(\Lambda-\lambda S_1+\mu S_1)\right\| \\ &\le \left\|-(\lambda+\mu)\right\|\left\|S(\chi)-S_1(\chi)\right\| \\ &\le \left\|-\left(\frac{\phi I}{N}+\frac{\phi D}{N}+\frac{\phi T}{N}+\mu\right)\right\|\left\|S(\chi)-S_1(\chi)\right\| \\ &\le \left(\phi\left\|\frac{I(\chi)}{N}\right\|+\phi\left\|\frac{D(\chi)}{N}\right\|+\phi\left\|\frac{T(\chi)}{N}\right\|+\mu\right)\left\|S(\chi)-S_1(\chi)\right\| \\ &\le (\phi M_3+\phi M_4+\phi M_5+\mu)\left\|S(\chi)-S_1(\chi)\right\| \\ &\le \phi_1\left\|S(\chi)-S_1(\chi)\right\|\end{aligned}$$

$\phi_1=(\phi M_3+\phi M_4+\phi M_5+\mu)$

Where; $M_1=\max_{\chi\in J}\|S(\chi)\|$, $M_2=\max_{\chi\in J}\|E(\chi)\|$, $M_3=\max_{\chi\in J}\|I(\chi)\|$, $M_4=\max_{\chi\in J}\|T(\chi)\|$,

$M_5=\max_{\chi\in J}\|D(\chi)\|$, $M_6=\max_{\chi\in J}\|R(\chi)\|$.

are bounded functions, we have

$\left\|\kappa_1(\chi,\ S(\chi))-\kappa_1(\chi,\ S_1(\chi))\right\| = \le \phi_1\left\|S(\chi)-S_1(\chi)\right\|$

Thus κ_1 satisfied the Lipschitz condition, and if $0\le\phi_1<1$, then it is also a contraction for κ_1. Similarly, the Lipschitz condition is satisfied by other kernels:

$$\left\|\kappa_2(\chi,\ E(\chi))-\kappa_2(\chi,\ E_1(\chi))\right\| = \le \phi_2\left\|E(\chi)-E_1(\chi)\right\|,$$

$$\left\|\kappa_3(\chi,\ I(\chi))-\kappa_3(\chi,\ I_1(\chi))\right\| = \le \phi_3\left\|I(\chi)-I_1(\chi)\right\|,$$

$$\left\|\kappa_4(\chi,\ T(\chi))-\kappa_4(\chi,\ T_1(\chi))\right\| = \le \phi_4\left\|T(\chi)-T_1(\chi)\right\|,$$

$$\left\|\kappa_5(\chi,\ D(\chi))-\kappa_5(\chi,\ D_1(\chi))\right\| = \le \phi_5\left\|D(\chi)-D_1(\chi)\right\|,$$

$$\left\|\kappa_6(\chi,\ R(\chi))-\kappa_6(\chi,\ R_1(\chi))\right\| = \le \phi_6\left\|R(\chi)-R_1(\chi)\right\|.$$

By considering the kernel for the model into account, we write (3) as follows :

$$S(\chi)=S(0)+\frac{1-\beta}{\mathrm{A}(\beta)}\kappa_1(\chi,\ S)+\frac{\beta}{\mathrm{A}(\beta)\Gamma(\chi)}\int_0^{\chi}(\chi-y)^{\beta-1}\kappa_1(\mathrm{y},\ S)\,dy,$$

$$E(\chi)=E(0)+\frac{1-\beta}{\mathrm{A}(\beta)}\kappa_2(\chi,\ E)+\frac{\beta}{\mathrm{A}(\beta)\Gamma(\chi)}\int_0^{\chi}(\chi-y)^{\beta-1}\kappa_2(\mathrm{y},\ E)\,dy,$$

$$I(\chi)=I(0)+\frac{1-\beta}{\mathrm{A}(\beta)}\kappa_3(\chi,\ I)+\frac{\beta}{\mathrm{A}(\beta)\Gamma(\chi)}\int_0^{\chi}(\chi-y)^{\beta-1}\kappa_3(\mathrm{y},\ I)\,dy,$$

$$T(\chi)=T(0)+\frac{1-\beta}{\mathrm{A}(\beta)}\kappa_4(\chi,\ T)+\frac{\beta}{\mathrm{A}(\beta)\Gamma(\chi)}\int_0^{\chi}(\chi-y)^{\beta-1}\kappa_4(\mathrm{y},\ T)\,dy,$$

$$D(\chi)=D(0)+\frac{1-\beta}{\mathrm{A}(\beta)}\kappa_5(\chi,\ D)+\frac{\beta}{\mathrm{A}(\beta)\Gamma(\chi)}\int_0^{\chi}(\chi-y)^{\beta-1}\kappa_5(\mathrm{y},\ D)\,dy,$$

$$R(\chi)=R(0)+\frac{1-\beta}{\mathrm{A}(\beta)}\kappa_6(\chi,\ R)+\frac{\beta}{\mathrm{A}(\beta)\Gamma(\chi)}\int_0^{\chi}(\chi-y)^{\beta-1}\kappa_6(\mathrm{y},\ R)\,dy. \qquad (4)$$

Therefore, presenting (4) recursively yields

$$S_v(\chi)=\frac{1-\beta}{\mathrm{A}(\chi)}\kappa_1(\chi,\ S_{v-1})+\frac{\beta}{\mathrm{A}(\beta)\Gamma(\chi)}+\int_0^{\chi}(\chi-y)^{\beta-1}\kappa_1(\mathrm{y},\ S_{v-1})\,dy,$$

$$E_v(\chi)=\frac{1-\beta}{\mathrm{A}(\chi)}\kappa_2(\chi,\ E_{v-1})+\frac{\beta}{\mathrm{A}(\beta)\Gamma(\chi)}+\int_0^{\chi}(\chi-y)^{\beta-1}\kappa_2(\mathrm{y},\ E_{v-1})\,dy,$$

$$I_v(\chi)=\frac{1-\beta}{\mathrm{A}(\chi)}\kappa_3(\chi,\ I_{v-1})+\frac{\beta}{\mathrm{A}(\beta)\Gamma(\chi)}+\int_0^{\chi}(\chi-y)^{\beta-1}\kappa_3(\mathrm{y},\ I_{v-1})\,dy,$$

$$T_v(\chi)=\frac{1-\beta}{\mathrm{A}(\chi)}\kappa_4(\chi,\ T_{v-1})+\frac{\beta}{\mathrm{A}(\beta)\Gamma(\chi)}+\int_0^{\chi}(\chi-y)^{\beta-1}\kappa_4(\mathrm{y},\ T_{v-1})\,dy,$$

$$D_v(\chi)=\frac{1-\beta}{\mathrm{A}(\chi)}\kappa_5(\chi,\ D_{v-1})+\frac{\beta}{\mathrm{A}(\beta)\Gamma(\chi)}+\int_0^{\chi}(\chi-y)^{\beta-1}\kappa_5(\mathrm{y},\ D_{v-1})\,dy,$$

$$R_v(\chi)=\frac{1-\beta}{\mathrm{A}(\chi)}\kappa_6(\chi,\ R_{v-1})+\frac{\beta}{\mathrm{A}(\beta)\Gamma(\chi)}+\int_0^{\chi}(\chi-y)^{\beta-1}\kappa_6(\mathrm{y},\ R_{v-1})\,dy.$$

Subject to the initial conditions:

$$S_0(\chi)=S(0),E_0(\chi)=E(0),I_0(\chi)=I(0),T(\chi)=T(0),D(\chi)=D(0),\ R_0(\chi)=R(0)$$

The system (5) is obtained by using the initial conditions and considering the difference between the successive terms.

$$\Psi_v(\chi)=S_v(\chi)-S_{v-1}(\chi)=\frac{1-\beta}{\mathrm{A}(\beta)}\kappa_1(\chi,\ S_{v-1})-\kappa_1(\chi,\ S_{v-2})$$
$$+\frac{\beta}{\mathrm{A}(\beta)\Gamma(\chi)}\int_0^{\chi}(\chi-y)^{\beta-1}\left(\kappa_1(\chi,\ S_{v-1})-\kappa_1(\chi,\ S_{v-2})\right)dy$$

$$\Phi_v(\chi)=E_v(\chi)-E_{v-1}(\chi)=\frac{1-\beta}{\mathrm{A}(\beta)}\kappa_2(\chi,\ E_{v-1})-\kappa_2(\chi,\ E_{v-2})$$
$$+\frac{\beta}{\mathrm{A}(\beta)\Gamma(\chi)}\int_0^{\chi}(\chi-y)^{\beta-1}\left(\kappa_2(\chi,\ S_{v-1})-\kappa_2(\chi,\ E_{v-2})\right)dy$$

$$\Delta_v(\chi)=I_v(\chi)-I_{v-1}(\chi)=\frac{1-\beta}{\mathrm{A}(\beta)}\kappa_3(\chi,\ I_{v-1})-\kappa_3(\chi,\ I_{v-2})$$
$$+\frac{\beta}{\mathrm{A}(\beta)\Gamma(\chi)}\int_0^{\chi}(\chi-y)^{\beta-1}\left(\kappa_3(\chi,\ I_{v-1})-\kappa_3(\chi,\ I_{v-2})\right)dy$$

$$\Upsilon_v(\chi)=T_v(\chi)-T_{v-1}(\chi)=\frac{1-\beta}{\mathrm{A}(\beta)}\kappa_4(\chi,\ T_{v-1})-\kappa_4(\chi,\ T_{v-2})$$
$$+\frac{\beta}{\mathrm{A}(\beta)\Gamma(\chi)}\int_0^{\chi}(\chi-y)^{\beta-1}\left(\kappa_4(\chi,\ T_{v-1})-\kappa_4(\chi,\ T_{v-2})\right)dy$$

$$\Omega_v(\chi)=D_v(\chi)-D_{v-1}(\chi)=\frac{1-\beta}{\mathrm{A}(\beta)}\kappa_5(\chi,\ D_{v-1})-\kappa_5(\chi,\ D_{v-2})$$
$$+\frac{\beta}{\mathrm{A}(\beta)\Gamma(\chi)}\int_0^{\chi}(\chi-y)^{\beta-1}\left(\kappa_4(\chi,\ D_{v-1})-\kappa_4(\chi,\ D_{v-2})\right)dy$$

$$\Xi_v(\chi) = R_v(\chi) - R_{v-1}(\chi) = \frac{1-\beta}{\mathrm{A}(\beta)}\kappa_6\left(\chi,\ R_{v-1}\right) - \kappa_6\left(\chi,\ R_{v-2}\right) + \frac{\beta}{\mathrm{A}(\beta)\Gamma(\chi)}\int_0^{\chi}\left(\chi - y\right)^{\beta-1}\left(\kappa_6\left(\chi,\ R_{v-1}\right) - \kappa_6\left(\chi,\ R_{v-2}\right)\right)dy \tag{5}$$

Where:

$$S_v(\chi) = \sum_{i=1}^{v}\Psi_i(\chi),$$

$$E_v(\chi) = \sum_{i=1}^{v}\Phi_i(\chi),$$

$$I_v(\chi) = \sum_{i=1}^{v}\Delta_i(\chi),$$

$$T_v(\chi) = \sum_{i=1}^{v}\Upsilon_i(\chi),$$

$$D_v(\chi) = \sum_{i=1}^{v}\Omega_i(\chi),$$

$$R_v(\chi) = \sum_{i=1}^{v}\Xi_i(\chi). \tag{6}$$

By considering the triangular inequality of equation (5). After applying the norm to equation (6), the equation is transformed into (7)

$$\begin{aligned}\left\|\Psi_v(\chi)\right\| &= \left\|S_v(\chi) - S_{v-1}(\chi)\right\| \\ &\le \frac{1-\beta}{\mathrm{A}(\beta)}\left\|\kappa_1\left(\chi,\ S_{v-1}\right) - \kappa_1\left(\chi,\ S_{v-2}\right)\right\| \\ &+ \frac{\beta}{\mathrm{A}(\beta)\Gamma(\chi)}\left\|\int_0^{\chi}\left(\chi - y\right)^{\beta-1}\left(\kappa_1\left(\chi,\ S_{v-1}\right) - \kappa_1\left(\chi,\ S_{v-2}\right)\right)dy\right\|\end{aligned} \tag{7}$$

As the Lipschitz condition is satisfied by the kernel, the following equations hold:

$$\left\|S_v(\chi) - S_{v-1}(\chi)\right\| \le \frac{1-\beta}{\mathrm{A}(\beta)}\phi_1\left\|S_{v-1}(\chi) - S_{v-2}(\chi)\right\| + \frac{\beta}{\mathrm{A}(\beta)\Gamma(\chi)}\phi_1\int_0^{\chi}\left(\chi - y\right)^{\beta-1}\left\|S_{v-1}(\chi) - S_{v-2}(\chi)\right\|dy$$

and

$$\left\|\Phi_v(\chi)\right\| \le \frac{1-\beta}{\mathrm{A}(\beta)}\phi_2\left\|\Phi_{v-1}(\chi)\right\| + \frac{\beta}{\mathrm{A}(\beta)\Gamma(\chi)}\phi_2\int_0^{\chi}\left(\chi - y\right)^{\beta-1}\left\|\Phi_{v-1}(\chi)\right\|dy$$

(8)

Similarly, we have the following results :

$$\left\|\Delta_v(\chi)\right\| \le \frac{1-\beta}{\mathrm{A}(\beta)}\phi_3\left\|\Delta_{v-1}(\chi)\right\| + \frac{\beta}{\mathrm{A}(\beta)\Gamma(\chi)}\phi_3\int_0^{\chi}\left(\chi - y\right)^{\beta-1}\left\|\Delta_{v-1}(\chi)\right\|dy$$

$$\left\|\Upsilon_v(\chi)\right\| \le \frac{1-\beta}{\mathrm{A}(\beta)}\phi_4\left\|\Upsilon_{v-1}(\chi)\right\| + \frac{\beta}{\mathrm{A}(\beta)\Gamma(\chi)}\phi_4\int_0^{\chi}\left(\chi - y\right)^{\beta-1}\left\|\Upsilon_{v-1}(\chi)\right\|dy$$

$$\left\|\Omega_v(\chi)\right\| \le \frac{1-\beta}{\mathrm{A}(\beta)}\phi_5\left\|\Omega_{v-1}(\chi)\right\| + \frac{\beta}{\mathrm{A}(\beta)\Gamma(\chi)}\phi_5\int_0^{\chi}\left(\chi - y\right)^{\beta-1}\left\|\Omega_{v-1}(\chi)\right\|dy$$

$$\left\|\Xi_{v}(\chi)\right\| \leq \frac{1-\beta}{\mathrm{A}(\beta)}\phi_{6}\left\|\Xi_{v-1}(\chi)\right\| + \frac{\beta}{\mathrm{A}(\beta)\Gamma(\chi)}\phi_{6}\int_{0}^{\chi}(\chi-y)^{\beta-1}\left\|\Xi_{v-1}(\chi)\right\|dy$$

Theorem 4.2. The COVID-19 model (2) with the ABC fractional order derivative has a unique solution if $\chi_{\max}$ satisfies the following condition

$$\frac{1-\beta}{\mathrm{A}(\beta)}\phi_{i} + \frac{\chi_{\max}}{\mathrm{A}(\beta)\Gamma(\chi)}\phi_{i} < 1, \qquad for\ \ i = 1,2,\ldots,6.$$

Proof.

It clear that $S(\chi), E(\chi), I(\chi), T(\chi), D(\chi), R(\chi)$ are bounded and the kernel of these functions also satisfied the Lipsachitz condition. Hence applying the succeeding relation with the application of equation (8) yields

$$\left\|\Psi_{v}(\chi)\right\| \leq \left\|S(0)\right\|\left[\frac{1-\beta}{\mathrm{A}(\beta)}\phi_{1} + \frac{\chi_{\max}}{\mathrm{A}(\beta)\Gamma(\chi)}\phi_{1}\right]^{v},$$

$$\left\|\Phi_{v}(\chi)\right\| \leq \left\|E(0)\right\|\left[\frac{1-\beta}{\mathrm{A}(\beta)}\phi_{2} + \frac{\chi_{\max}}{\mathrm{A}(\beta)\Gamma(\chi)}\phi_{2}\right]^{v},$$

$$\left\|\Delta_{v}(\chi)\right\| \leq \left\|I(0)\right\|\left[\frac{1-\beta}{\mathrm{A}(\beta)}\phi_{3} + \frac{\chi_{\max}}{\mathrm{A}(\beta)\Gamma(\chi)}\phi_{3}\right]^{v},$$

$$\left\|\Upsilon_{v}(\chi)\right\| \leq \left\|T(0)\right\|\left[\frac{1-\beta}{\mathrm{A}(\beta)}\phi_{4} + \frac{\chi_{\max}}{\mathrm{A}(\beta)\Gamma(\chi)}\phi_{4}\right]^{v},$$

$$\left\|\Omega_{v}(\chi)\right\| \leq \left\|D(0)\right\|\left[\frac{1-\beta}{\mathrm{A}(\beta)}\phi_{5} + \frac{\chi_{\max}}{\mathrm{A}(\beta)\Gamma(\chi)}\phi_{5}\right]^{v},$$

$$\left\|\Xi_{v}(\chi)\right\| \leq \left\|R(0)\right\|\left[\frac{1-\beta}{\mathrm{A}(\beta)}\phi_{6} + \frac{\chi_{\max}}{\mathrm{A}(\beta)\Gamma(\chi)}\phi_{6}\right]^{v}.$$

Hence, since equation (6) is a smooth function and it exists.

$$S(\chi) - S(0) = S_{v}(\chi) - \Psi_{1(v)}(\chi)$$

$$E(\chi) - E(0) = E_{v}(\chi) - \Psi_{2(v)}(\chi)$$

$$I(\chi) - I(0) = I_{v}(\chi) - \Psi_{3(v)}(\chi)$$

$$T(\chi) - T(0) = T_{v}(\chi) - \Psi_{4(v)}(\chi)$$

$$D(\chi) - D(0) = D_{v}(\chi) - \Psi_{5(v)}(\chi)$$

$$R(\chi) - R(0) = R_{v}(\chi) - \Psi_{6(v)}(\chi)$$

The term $\left\|\Psi_{\infty}(\xi)\right\| \to 0$ at infinity

$$\left\|\Psi_{\infty}(\chi)\right\| \leq \left\|\frac{1-\beta}{\mathrm{A}(\beta)}\kappa_{1}(\chi,\ S) - \kappa_{1}(\chi,\ S_{v-1}) + \frac{\beta}{\mathrm{A}(\beta)\Gamma(\chi)}\int_{0}^{\chi}(\chi-y)^{\beta-1}\left(\kappa_{1}(\chi,\ S) - \kappa_{1}(\chi,\ S_{v-1})\right)dy\right\|$$

$$\left\|\Psi_{\infty}(\chi)\right\| \leq \frac{1-\beta}{\mathrm{A}(\beta)}\left\|\kappa_{1}(\chi,\ S) - \kappa_{1}(\chi,\ S_{v-1})\right\| + \frac{\beta}{\mathrm{A}(\beta)\Gamma(\chi)}\int_{0}^{\chi}(\chi-y)^{\beta-1}\left\|\kappa_{1}(\chi,\ S) - \kappa_{1}(\chi,\ S_{v-1})\right\|dy$$

$$\leq \frac{1-\beta}{\mathrm{A}(\beta)}\phi_1\left\|S-S_{v-1}\right\|+\frac{\chi^{\beta}}{\mathrm{A}(\beta)\Gamma(\chi)}\phi_1\left\|S_v-S_{v-1}\right\|$$

By recursively repeating the process, yields

$$\left\|\Psi_{\infty}(\chi)\right\|\leq\left[\frac{1-\beta}{\mathrm{A}(\beta)}+\frac{\chi^{\beta}}{\mathrm{A}(\beta)\Gamma(\chi)}\phi_1\right]^{v+1}\phi_1^{v}M$$

Apply $\chi_{\max}$, we have

$$\left\|\Psi_{\infty}(\chi)\right\|\leq\left[\frac{1-\beta}{\mathrm{A}(\beta)}+\frac{\chi^{\beta}{}_{\max}}{\mathrm{A}(\beta)\Gamma(\chi)}\phi_1\right]^{v+1}\phi_1^{v}M$$

Taking the limit on both sides as $v\to\infty,$ we havs $\left\|\Psi_{\infty}(\chi)\right\|\to 0$

4.1 Uniqueness of Solution

Showing that the system has a unique solution is an important part of understanding how it behaves. To explore this, we use the idea of contraction and assume, for the sake of argument, that there might be a second possible solution to system (2).

$S_1(\chi), E_1(\chi), I_1(\chi), T_1(\chi), D_1(\chi), R_1(\chi)$

$$\left\|S(\chi)-S_1(\chi)\right\|\leq\frac{1-\beta}{\mathrm{A}(\beta)}\left(\kappa_1(\chi,\ S)-\kappa_1(\chi,\ S_1)\right)+\frac{\beta}{\mathrm{A}(\beta)\Gamma(\chi)}\int_0^{\chi}(\chi-y)^{\beta-1}\left(\kappa_1(\chi,\ S)-\kappa_1(\chi,\ S_1)\right)dy \quad (9)$$

Applying the norm to equation (9)

$$\left\|S(\chi)-S_1(\chi)\right\|\leq\frac{1-\beta}{\mathrm{A}(\beta)}\left\|\kappa_1(\chi,\ S)-\kappa_1\left(\chi,\ S_{1}\right)\right\|+\frac{\beta}{\mathrm{A}(\beta)\Gamma(\chi)}\int_0^{\chi}(\chi-y)^{\beta-1}\left\|\kappa_1(\chi,\ S)-\kappa_1(\chi,\ S_1)\right\|dy,$$

Applying the kernel's Lipchitz conditional properties, obtain

$$\leq\frac{1-\beta}{\mathrm{A}(\beta)}\left\|S(\chi)-S_1(\chi)\right\|\phi_1+\frac{\phi_1\chi^{\beta}}{\mathrm{A}(\beta)\Gamma(\chi)}\left\|S(\chi)-S_1(\chi)\right\|,\ \text{yields}$$

$$\left\|S(\chi)-S_1(\chi)\right\|\left(1-\phi_1\frac{1-\beta}{\mathrm{A}(\beta)}+\frac{\phi_1\chi^{\beta}}{\mathrm{A}(\beta)\Gamma(\chi)}\right)\leq 0,$$

$$\left\|S(\chi)-S_1(\chi)\right\|=0\to S(\chi)=S_1(\chi)$$

Hence , the system has a unique solution. Similarly, the above result can be obtained for various solutions of $E(\chi), I(\chi), T(\chi), T(\chi), R(\chi).$

4.2 The Basic Reproduction Number (R_0)

The basic reproduction number (R_0), often referred to as represents the average number of new infections generated by a single individual with COVID-19 during their infectious period, assuming the entire population is susceptible. This key metric helps assess how contagious the disease is under ideal conditions. To determine (R_0) we apply the next-generation matrix method to our dynamical system, as outlined in [23, 35]. Using this approach, we derive the following expression for the basic reproduction number:

$R_0=\rho\left(FV^{-1}\right)$ where ρ is the dominant eigenvalue of FV^{-1}

$$F=\begin{bmatrix}0 & \phi & \phi & \phi\\ 0 & 0 & 0 & 0\\ 0 & 0 & 0 & 0\\ 0 & 0 & 0 & 0\end{bmatrix}, V=\begin{bmatrix}K_1 & 0 & 0 & 0\\ -\varepsilon_1 & K_2 & 0 & 0\\ 0 & -\alpha_1 & \alpha_2 & -\alpha_1\\ 0 & -\omega & 0 & K_3\end{bmatrix},$$

$$FV^{-1}=\begin{bmatrix}\frac{\phi\varepsilon_1}{K_1K_2}+\frac{\phi\alpha_1\varepsilon_1(\omega+K_3)}{K_1K_2\alpha_2K_3}+\frac{\phi\omega\varepsilon_1}{K_1K_2K_3} & \frac{\phi}{K_2}+\frac{\phi\alpha_1(\omega+K_3)}{K_2\alpha_2K_3}+\frac{\phi\omega}{K_1K_2} & \frac{\phi}{\alpha_2} & \frac{\phi\alpha_1}{\alpha_2K_3}+\frac{\phi}{K_3}\\ 0 & 0 & 0 & 0\\ 0 & 0 & 0 & 0\\ 0 & 0 & 0 & 0\end{bmatrix}$$

$$R_0=\frac{\phi\varepsilon_1\left(\omega\alpha_1+\omega\alpha_2+K_3\alpha_1+K_3\alpha_2\right)}{K_1K_2\alpha_2K_3}$$ Where $K_1=(\varepsilon_1+\mu)$ $K_2=(\alpha_1+\omega+\mu)$ $K_3=(\alpha_1+\mu)$

4.3 Local Asymptotic Stability of the DFE of the Model

In dynamical system modeling, local stability refers to how a system behaves in the vicinity of an equilibrium or steady state [22, 23]. Analyzing local stability is essential for understanding whether small disturbances will fade away or grow over time near that point. This type of analysis plays a vital role across multiple disciplines, including physics, biology, economics, and engineering.

Theorem 4.3

The disease-free equilibrium point of the model is locally asymptotically stable (LAS) if $R_0<1$, *and unstable if* $R_0>1$.

Proof

To determine the local stability of the disease-free equilibrium, the Jacobian matrix is employed.

$$J\left(\varepsilon_0\right)=\begin{bmatrix}-\mu & 0 & -\phi & -\phi & -\phi & 0\\ 0 & -K_1 & \phi & \phi & \phi & 0\\ 0 & \varepsilon_1 & -K_2 & 0 & 0 & 0\\ 0 & 0 & \alpha_1 & -\alpha_2 & \alpha_1 & 0\\ 0 & 0 & \omega & 0 & -K_3 & 0\\ 0 & 0 & 0 & 0 & \gamma & -\mu\end{bmatrix}$$

As the first and last columns contain only their respective diagonal entries, the matrix can be reduce $J\left(\varepsilon_0\right)$to

$$J_1(\varepsilon_0)=\begin{bmatrix} -K_1 & \phi & \phi & \phi \\ \varepsilon_1 & -K_2 & 0 & 0 \\ 0 & \alpha_1 & -\alpha_2 & \alpha_1 \\ 0 & \omega & 0 & -K_3 \end{bmatrix}$$

The characteristics polynomial of $J_1(\varepsilon_0)$ is given below

$$\lambda^4+(K_3+\alpha_2+K_2+K_1)\lambda^3+(-\varepsilon_1\phi+K_2K_1+K_3K_1+\alpha_2K_1+K_3K_2+\alpha_2K_2+K_3\alpha_2)\lambda^2$$
$$+(-\omega\varepsilon_1\phi-\phi K_3\varepsilon_1-\alpha_1\varepsilon_1\phi-\phi\alpha_2\varepsilon_1+K_1K_2K_3+K_1K_2\alpha_2+K_1K_3\alpha_2+K_2K_3\alpha_2)\lambda$$
$$-\omega\varepsilon_1\phi\alpha_1-\omega\varepsilon_1\phi\alpha_2-\phi K_3\alpha_1\varepsilon_1-\phi K_3\alpha_2\varepsilon_1+K_1K_2\alpha_2K_3$$
$$\lambda^4+(K_3+\alpha_2+K_2+K_1)\lambda^3+(-\varepsilon_1\phi+K_2K_1+K_3K_1+\alpha_2K_1+K_3K_2+\alpha_2K_2+K_3\alpha_2)\lambda^2$$
$$+(-\omega\varepsilon_1\phi-\phi K_3\varepsilon_1-\alpha_1\varepsilon_1\phi-\phi\alpha_2\varepsilon_1+K_1K_2K_3+K_1K_2\alpha_2+K_1K_3\alpha_2+K_2K_3\alpha_2)\lambda$$
$$+K_1K_2\alpha_2K_3\left(1-\frac{\phi\varepsilon_1(\omega\alpha_1+\omega\alpha_2+K_3\alpha_1+K_3\alpha_2)}{\alpha_2K_1K_2K_3}\right)$$
$$\lambda^4+(K_3+\alpha_2+K_2+K_1)\lambda^3+(-\grave{o}_1\phi+K_2K_1+K_3K_1+\alpha_2K_1+K_3K_2+\alpha_2K_2+K_3\alpha_2)\lambda^2$$
$$+(-\omega\varepsilon_1\phi-\phi K_3\varepsilon_1-\alpha_1\varepsilon_1\phi-\phi\alpha_2\varepsilon_1+K_1K_2K_3+K_1K_2\alpha_2+K_1K_3\alpha_2+K_2K_3\alpha_2)\lambda$$
$$+K_1K_2\alpha_2K_3(1-R_0)$$

Employing the Routh-Hurwitz method on the characteristic polynomial [6], we determine that

$$(1-R_0)>0$$
$$R_0<1$$

Based on the analysis conducted using the Jacobian matrix and the application of the Routh-Hurwitz stability criterion to the characteristic polynomial, it is established that all the eigenvalues associated with the linearized system at the disease-free equilibrium (DFE) have negative real parts. This implies that small perturbations or deviations from the DFE will decay over time, and the system will return to its equilibrium state [27, 28, 29]. Therefore, the disease-free equilibrium point of the proposed model is locally asymptotically stable, indicating that in the absence of external disturbances or reinfections, the infection will eventually be eradicated from the population.

5.0 Numerical Simulations.

Table 2. Parameter used for simulations

Parameter	Value	Source
Λ	$\frac{10000}{59\times365}$	Estimated
μ	0.5500	Assumed
ϕ	0.6000	[23]
γ	0.106	Assumed
α_1	0.150	[23]
ε_1	0.25	Assumed
α_2	0.2000	[23]
ω	0.9700	[23]

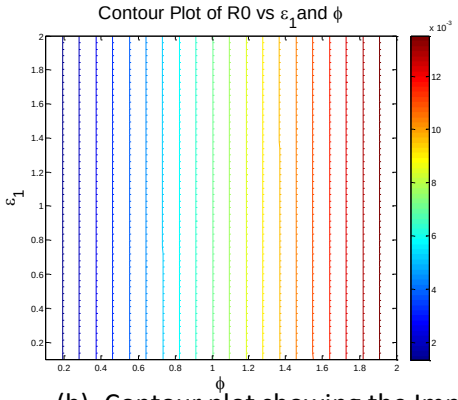

(b) Contour plot showing the Impact Of ε_1 and ϕ on R_0

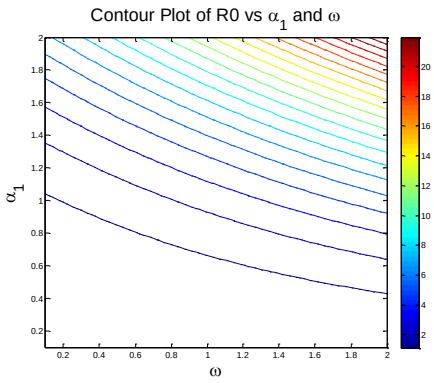

(a) Contour plot showing the Impact Of ω and α_1 on R_0

Fig 3: Basic reproduction number contour plot

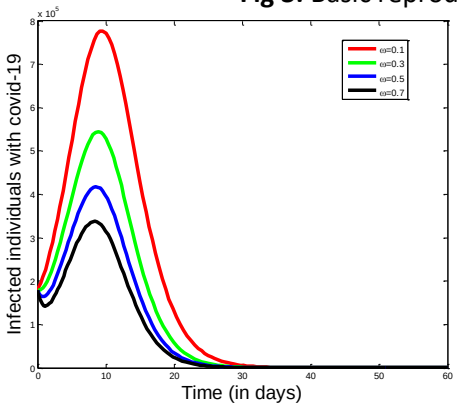

(a) Simulation of infected Humans with Covid-19

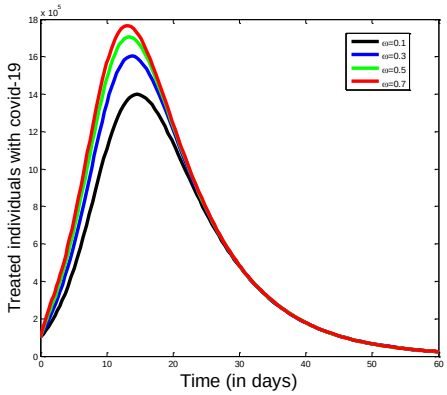

(b) Simulation of treated Humans with Covid-19

Fig 4: Effect of ω on $I(t)$ and $T(t)$

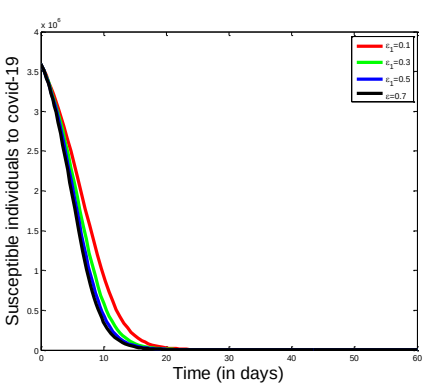

(a) Simulation of infected Humans with Covid-19

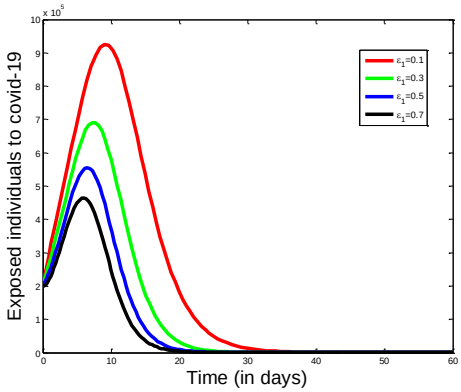

(b) Simulation of treated Humans with Covid-19

Fig 5: Effect of ε_1 on $S(t)$ and $E(t)$

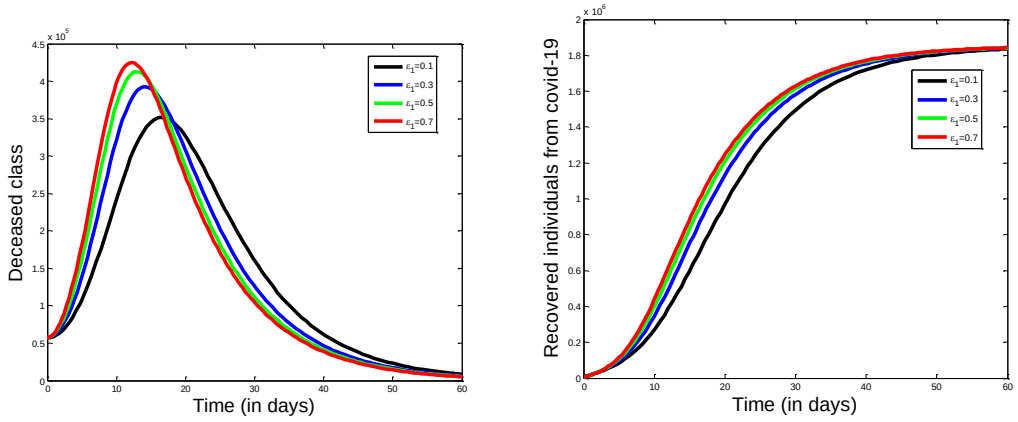

(a) Simulation of Covid-19 Deceased individuals

(b) Simulation of Recovered individuals from Covid-19

Fig 6: Effect of ε_1 on $D(t)$ and $R(t)$

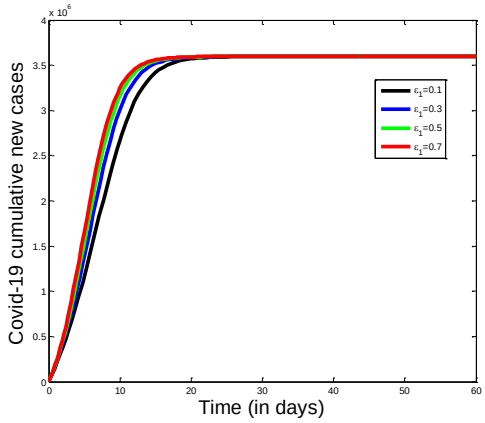

Fig 7: covid-19 cumulative new cases

Figure 3a shows the surface plot of R_0 as a function of the progression rate ε_1 and the contact rate ϕ. As ϕ increases in the plot, R_0 increases as well, since more frequent contacts lead to more opportunities for transmission. As ε_1 increases, R_0 also increases because individuals that progress to the infectious stage more quickly, contributing to more secondary cases. The contour lines in this plot likely slope upward to the right, indicating that simultaneous increases in both ϕ and ε_1 lead to an even higher R_0. If both parameters are high, the disease spreads more quickly in the population. **Figure 3b** depicts how R_0 depends on the treatment rate ω and the disease-induced death rate α_1. as ω increases, R_0 decreases in the plot, as more treatment means infected individuals are removed from the infectious pool more quickly, reducing transmission. as α_1 increases, R_0 also decreases because deaths remove infectious individuals from the population, limiting further spread. In the plot, the contour lines likely slope downward to the right, showing that higher values of either ω or α_1 correspond to a reduced value of R_0. If both parameters are high, the disease's potential to

spread is even lower. Figure 4 illustrates the number of infected individuals over time. At lower treatment rate, the infection curve rises sharply, indicating a rapid and uncontrolled spread of the disease. The number of infected people reaches a high peak before gradually declining, likely due to natural recovery, the development of immunity, or the depletion of susceptible individuals. As the treatment rate increases, the peak becomes noticeably lower and occurs earlier, demonstrating that timely and effective treatment can disrupt the transmission chain. At sufficiently high treatment rates, the infection curve flattens significantly, suggesting that most infected individuals are quickly moved into the treated class before they can further spread the disease.

The second part of Figure 4 depicts the treated population. At low treatment rates, the number of treated individuals increases slowly and reaches only a modest peak. However, with higher treatment rate, this number grows more rapidly and reaches higher values. This reflects more efficient identification and treatment of infected individuals, reducing the disease burden. Notably, for higher treatment rates, the treated population peaks earlier and at greater levels, indicating a quicker and more effective response by the healthcare system or treatment intervention modeled. Figure 5a shows that as the progression rate (ε_1) increases, the susceptible population declines more rapidly. This is because individuals transition more quickly from the exposed class to the infected class, accelerating the depletion of the susceptible population as the infection spreads more efficiently. Figure 5b demonstrates that an increase in the progression rate (ε_1) results in a sharper and more pronounced peak in the exposed population. The rapid transition from exposure to infection causes the exposed group to peak earlier and decline faster. In Figure 6a, the graph of deceased individuals reveals that higher progression rates accelerate the growth of this group. This is due to the faster transition into the infected class, leading to more individuals reaching the stage where death can occur, and doing so both sooner and in larger numbers. Figure 6b, which shows the recovered population, follows a similar trend to the infected class: a higher progression rate (ε_1) leads to a quicker rise in recoveries. Since more individuals become infected sooner, the recovery process also begins earlier and peaks more rapidly. Finally, Figure 7 presents the graph of cumulative new cases. As the progression rate (ε_1) increases, the curve becomes steeper and peaks earlier. This reflects a more intense and abrupt outbreak, as the faster movement from exposure to infection accelerates the rate at which new cases are recorded.

Conclusion

This study presents a fractional-order compartmental model using the Atangana–Baleanu–Caputo derivative to analyze the transmission dynamics of COVID-19. By incorporating memory effects, the model provided a more realistic representation of the disease's progression compared to classical integer-order models. Stability analysis confirmed that the disease-free equilibrium is locally asymptotically stable when the basic reproduction number is less than one. Numerical simulations demonstrated that reducing the contact rate and enhancing treatment accessibility significantly decreased infection levels and boosted recovery rates. The findings underscore the critical importance of early intervention, behavioural controls, and accessible treatment in managing the spread of COVID-19. The proposed model not only offers valuable insights into current pandemic control but also serves as a robust framework for addressing future infectious disease outbreaks characterized by memory-dependent dynamics.

References

1. Patel, M., Joshi, R., & Deshmukh, S. (2025). Rising COVID-19 cases in urban hospitals: A Pune study. *Journal of Infectious Diseases and Public Health*, 18(1), 45–53. https://doi.org/10.1016/j.jiph.2024.12.002
2. Smith, J. R., Nguyen, H. T., Lee, S. Y., & Williams, D. (2025). Interim estimates of COVID-19 vaccine effectiveness during 2024-2025. *MMWR Morbidity and Mortality Weekly Report*, 74, 123–128. https://doi.org/10.15585/mmwr.mm7406a1
3. Kumar, S., Verma, A., Singh, P., & Sharma, R. (2025). COVID-19 recovery trends in Madhya Pradesh, India. *International Journal of Epidemiology*, 54(2), 200–208. https://doi.org/10.1093/ije/dyad015
4. Chen, L., Johnson, T. M., Garcia, R., & Thompson, M. (2025). CDC vaccine guidelines update and expert opinions in Connecticut. *Vaccine*, 43(5), 899–904. https://doi.org/10.1016/j.vaccine.2024.12.021
5. Jackson, T. L., Nguyen, P. T., Brown, K. A., & Miller, D. (2025). COVID-19 booster shot uptake in Australia: A public health perspective. *Australian and New Zealand Journal of Public Health*, 49(3), 247–254. https://doi.org/10.1111/1753-6405.13459
6. Wong, C., Patel, A., Singh, N., & Lee, J. H. (2024). Long COVID impacts on quality of life in the UK. *The Lancet Respiratory Medicine*, 12(9), 789–798. https://doi.org/10.1016/S2213-2600(24)00275-3
7. Xu, X., Li, Y., Wang, J., & Chen, H. (2025). COVID-19 epidemiology and insights for 2023: A review. *Frontiers in Public Health*, 13, 114567. https://doi.org/10.3389/fpubh.2025.114567
8. Garcia-Beltran, W. F., Lam, E. C., St. Denis, K., Nitido, A. D., Garcia, Z. H., Hauser, B. M., Feldman, J., Pavlovic, M. N., Gregory, D. J., Poznansky, M. C., Sigal, A., Schmidt, A. G., Iafrate, A. J., Naranbhai, V., & Balazs, A. B. (2024). Effectiveness of updated COVID-19 vaccines against XBB.1.5 subvariant. *Nature Medicine*, 30(4), 725–733. https://doi.org/10.1038/s41591-024-01517-6
9. Baker, M. G., Fidler, D. P., & Wilson, N. (2025). Who should receive COVID-19 boosters? An evolving consensus. *Health Affairs*, 44(3), 399–406. https://doi.org/10.1377/hlthaff.2024.0185
10. Rogers, J. P., Watson, C. J., Badenoch, J., Cross, B., Butler, M. S., Song, J., Packer, R. J., Lewis, G., D'Mello, S., Evans, A., Pritchard, M., Hughes, C., & David, S. (2025). Organ failure linked to long COVID: Pathophysiology and clinical implications. *The New England Journal of Medicine*, 392(10), 987–997. https://doi.org/10.1056/NEJMoa2511323
11. Prather, K. A., Marr, L. C., Schooley, R. T., McDiarmid, M. A., Wilson, M. E., & Milton, D. K. (2023). Alternative transmission routes of COVID-19: A narrative review. *Journal of Infection*, 87(6), 712–723. https://doi.org/10.1016/j.jinf.2023.04.012
12. Centers for Disease Control and Prevention (CDC). (2024). Use of additional COVID-19 vaccine doses in adults aged 65 and older. *MMWR Morbidity and Mortality Weekly Report*, 73(49), 1118–1123. https://doi.org/10.15585/mmwr.mm7349a2
13. Harvey, W. T., Carabelli, A. M., Jackson, B., Gupta, R. K., Thomson, E. C., Harrison, E. M., Ludden, C., Reeve, R., Rambaut, A., Peacock, S. J., & Robertson, D. L. (2023). SARS-CoV-2 variants, spike mutations and immune escape. *Nature Reviews Microbiology*, 21, 387–401. https://doi.org/10.1038/s41579-023-00878-2
14. Goldman, E. (2023). Infectious life of COVID-19 on surfaces and fabrics: A review. *Journal of Hospital Infection*, 125, 10–18. https://doi.org/10.1016/j.jhin.2023.02.004

15. Liang, J., Xu, Y., Chen, C., & Liu, H. (2024). What you need to know about the 2024-2025 COVID-19 vaccines. *Vaccine*, 42(32), 4355–4362. https://doi.org/10.1016/j.vaccine.2024.05.004
16. Peterson, J. M., Nguyen, P., Sullivan, B., & Williams, R. (2025). Effectiveness of a single mRNA vaccine dose in previously infected individuals. *Communications Medicine*, 5, 151. https://doi.org/10.1038/s43856-025-00151-x
17. Nalbandian, A., Sehgal, K., Gupta, A., Madhavan, M. V., McGroder, C., Stevens, J. S., Cook, J. R., Nordvig, A. S., Shalev, D., Sehrawat, T. S., Ahluwalia, N., Bikdeli, B., Dietz, D., Der-Nigoghossian, C., Liyanage-Don, N., Rosner, G. F., Bernstein, E. J., Mohan, S., Beckley, A. A., & Wan, E. Y. (2023). Post-acute COVID-19 syndrome (Long COVID): A review of clinical characteristics and pathogenesis. *Nature Reviews Disease Primers*, 9(1), 41. https://doi.org/10.1038/s41572-023-00387-4
18. Corti, D., Purcell, L. A., Snell, G., & Veesler, D. (2025). The future of vaccines: Needle-free delivery systems. *Nature Reviews Immunology*, 25, 211–223. https://doi.org/10.1038/s41577-025-00647-9
19. Andrews, N., Stowe, J., Kirsebom, F., Toffa, S., Rickeard, T., Gallagher, E., Gower, C., Kall, M., Groves, N., O'Connell, A.-M., Simons, D., Blomquist, P. B., Zaidi, A., Nash, S., Indalao, I., Lopez-Bernal, J., Dunachie, S., Byers, C., Myers, R., & Ramsay, M. (2024). COVID-19 vaccine effectiveness against JN.1 subvariant. *The Lancet Infectious Diseases*, 24(3), 307–314. https://doi.org/10.1016/S1473-3099(24)00045-7
20. Murthy, S., Farooqui, M., Lee, K., & Gupta, R. (2024). Effectiveness of 2023–2024 COVID-19 vaccine formula in working-aged adults. *Cleveland Clinic Journal of Medicine*, 91(7), 394–402. https://doi.org/10.3949/ccjm.91a.23032
21. Anderson, R. M., & May, R. M. (2023). Early transmission dynamics and modeling of COVID-19. *Preventing Chronic Disease*, 20, 230089. https://doi.org/10.5888/pcd20.230089
22. Agbata, B. C., Omale, D., Ojih, P. B., & Omatola, I. U. (2019). Mathematical analysis of chickenpox transmission dynamics with control measures. *Continental Journal of Applied Sciences, 14*(2), 6–23. https://www.researchgate.net/publication/344234584
23. Agbata, B. C., Shior, M. M., Obeng-Denteh, W., Omotehinwa, T. O., Paul, R. V., Kwabi, P. A., & Asante-Mensa, F. (2023). A mathematical model of COVID-19 transmission dynamics with effects of awareness and vaccination program. *Journal of Ghana Science Association, 21*(2), 59–61. https://www.researchgate.net/publication/379485392_
24. Atangana, A., &Baleanu, D. (2016). New fractional derivatives with nonlocal and nonsingular kernel: Theory and application to heat transfer model. *Thermal Science*, 20(3), 763-769. https://doi.org/10.2298/TSCI160111018A
25. Atangana, A., &Goufo, E. F. D. (2023). Network-based fractional-order epidemic models with impulsive control strategies. *Chaos, Solitons& Fractals*, 172, 113888.https://doi.org/10.1016/j.chaos.2023.113888
26. Mahmood, H., Khan, N., & Ahmad, S. (2023). Modeling tuberculosis dynamics using Caputo fractional derivatives and the homotopy perturbation method.Bulletin of the National Research Centre, 47(1), 58.https://doi.org/10.1186/s42269-023-00872-1
27. Acheneje, G. O., Omale, D., Agbata, B. C., Atokolo, W., Shior, M. M., & Bolawarinwa, B. (2024). Approximate solution of the fractional order mathematical model on the transmission dynamics of the co-infection of COVID-19 and Monkeypox using the Laplace-Adomian decomposition method. *International Journal of Mathematics and Statistics Studies, 12*(3), 17–51. https://eajournals.org/ijmss/vol12-issue-3-

28. Agbata, B. C., Agbebaku, D. F., Odo, C. E., Ojih, J. T., Shior, M. M., & Ezugorie, I. G. (2024). A mathematical model for the transmission dynamics of COVID-19 in Nigeria and its post-effects. *International Journal of Mathematical Analysis and Modelling*, *7*(2), 523–547. https://tnsmb.org/journal/index.php/ijmam/article/view/191
29. Agbata, B. C., Obeng-Denteh, W., Amoah-Mensah, J., Kwabi, P. A., Shior, M. M., Asante-Mensa, F., & Abraham, S. (2024). Numerical solution of fractional order model of measles disease with double dose vaccination. *Dutse Journal of Pure and Applied Sciences (DUJOPAS)*, *10*(3b), 202–217. https://www.ajol.info/index.php/dujopas/article/view/281624
30. Abdoon, M. M., & Alzahrani, E. O. (2024). A comparative study of fractional derivatives in modeling influenza transmission. *Applied Mathematics and Computation*, *449*, 128001. https://doi.org/10.1016/j.amc.2023.128001
31. Deressa, T. T., & Duressa, T. F. (2021). Fractional-order SEAIR epidemic model with optimal control using the Atangana–Baleanu–Caputo derivative. *AIMS Mathematics*, *6*(12), 13267–13290. https://doi.org/10.3934/math.2021719
32. Farman, M., Khan, M. A., Shah, K., & Atangana, A. (2022). Fractal-fractional analysis of a Zika virus model via ABC Caputo derivative with real data simulation. *Alexandria Engineering Journal*, *61*(11), 10973–10989. https://doi.org/10.1016/j.aej.2022.02.022
33. Abioye, A. I., Peter, O. J., Ogunseye, H. A., Oguntolu, F. A., Ayoola, T. A., & Oladapo, A. O. (2023). A fractional-order mathematical model for malaria and COVID-19 co-infection dynamics using the Atangana–Baleanu–Caputo derivative. *Results in Applied Mathematics*, *18*, 100343. https://doi.org/10.1016/j.rinam.2023.100343
34. Here's the complete APA-style reference for the specified article, including author list and link to its ResearchGate page:
35. **Agbata, B. C., Dervishi, R., Asante-Mensa, F., Kwabi, P. A., Odeh, J. O., Amoah-Mensah, J., Meseda, P. K., & Obeng-Deng-Denteh, W. (2025). Mathematical modelling of measles disease with double dose vaccination.** *Journal of Basic and Applied Science Research*, ***3*****(3), 199–214. https://dx.doi.org/10.4314/jobasr.v3i3.22**